# A Novel Self-Healing Methodology for RF Amplifier Circuits Based on Oscillation Principles

Abhilash Goyal, Madhavan Swaminathan and Abhijit Chatterjee
School of Electrical and Computer Engineering, Georgia Institute of Technology, Atlanta, GA-30332, USA

***Abstract*— This paper proposes a novel self-healing methodology for embedded RF Amplifiers (LNAs) in RF sub-systems. The proposed methodology is based on oscillation principles in which the Device-under-Test (DUT) itself generates the output test signature with the help of additional circuitry. The self-generated test signature from the DUT is analyzed by using on-chip resources for testing the LNA and controlling its calibration knobs to compensate for multi-parameter variations in the LNA manufacturing process. Thus, the proposed methodology enables self-test and self-calibration of RF circuits without the need for external test stimulus. The proposed methodology is demonstrated through simulations as well as measurements performed on a RF LNA.**

## I. INTRODUCTION

In the last decade, advances in integrated circuit (IC) technology have enabled integration of RF front-ends with multiple analog and digital functions on a single chip. To enable speed and device density advantages, CMOS technology has evolved from 250 nm device feature size to 22 nm. However, there are discouraging predictions regarding the effects of process variations on the yield of CMOS ICs for geometries below 100 nm [1], [2]. In very deep-submicron CMOS processes, RF circuits are expected to be increasingly prone to process variations, suffering from significant loss of parametric yield.

In the past, calibration methods for improving the manufacturing yield of RF subsystems, namely embedded LNAs, have been proposed in [3], [4]. In these methods, an input stimulus is applied to calibrate the embedded LNA and the output response is captured using embedded sensors. With the help of on-chip circuit resources, the tuning "knobs" of the LNA are adjusted to compensate for performance loss due to process variability effects. Although the method of [3], [4] helps in improving the yield of RF sub-systems by tuning the embedded LNA, both of these methods assume the availability of an RF-signal source (Fig. 1). In addition, loop-back of the transmitter output to the receiver input is necessary for testing the receiver, making the testing process cumbersome. Further, the RF stimulus source (the RF transmitter) needs to be tested first, before testing the embedded LNA.

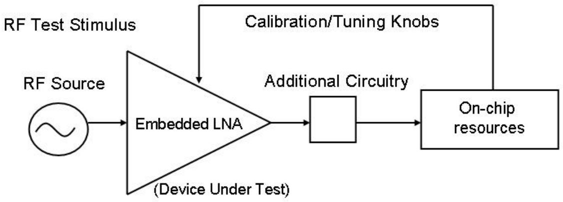

Fig 1. Prior self-calibration/healing methods [3], [4].

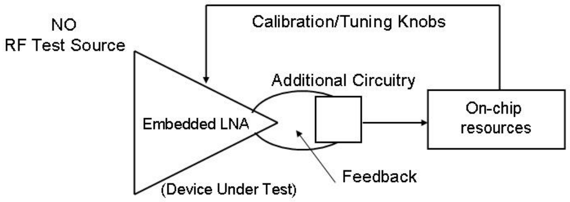

Fig. 2. Proposed self-healing architecture.

In this paper, a novel self-healing methodology is proposed for overcoming the need for external RF test stimulus. The proposed technique does not require the use of external test stimulus for performing self-healing because the stimulus is generated by the DUT itself with the help of additional circuitry using oscillation principles. This stimulus is used to assess the impact of process variations on the performance of the DUT. Subsequently, compensation for loss of DUT performance due to process variations is performed by adjusting calibration/tuning knobs designed into the DUT. This calibration knob manipulation is driven by analysis of the self-generated output (referred to as the DUT *signature*) from the DUT as shown in Fig. 2. The output signature of the DUT is analyzed with on-chip available resources (RF mixer, ADC and DSP). Thus, the proposed method enables self-test as well as self-correction of the embedded LNA leading to truly *self-healing* RF designs. In the past, oscillation based built-in self test (BIST) has been proposed for analog/mixed-signal active circuits in [5]. The method of [5] discusses only the testing aspects of analog/mixed-signal active circuits and does not introduce the concept of self-correction/calibration. The proposed methodology in this paper is also based on oscillation principles, but for the first time, a methodology for self-correction/calibration of active circuits such as an embedded RF LNA has been demonstrated.

In the following sections, the proposed self-healing methodology is discussed. Also, the self-healing LNA architecture and generation of calibration signals for tuning the calibration knobs is described. Simulation and measurement results are then presented.

## II. NOVEL SELF-HEALING METHODLOGY

### A). Self-Healing Flow

The overall self-healing methodology is shown in Fig. 3. After fabrication, the DUT is tested to identify those DUTs with catastrophic vs. parametric defects. The proposed self-healing procedure is exercised only if the DUT is determined to be free of catastrophic faults.

978-3-9810801-5-5/DATE09 © 2009 EDAA

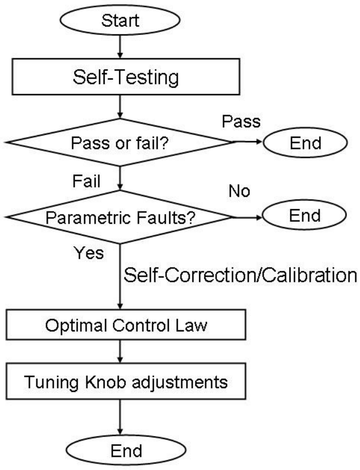

Fig. 3. Self-healing flow.

### B). Self-Healing Architecture

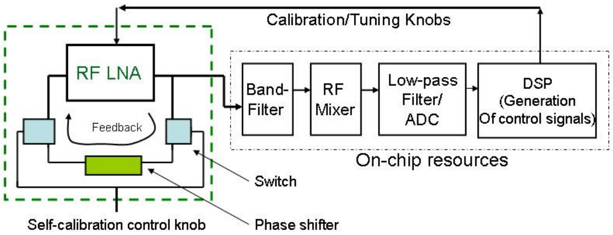

Fig. 4. Proposed self-healing LNA architecture.

Consider the proposed self-healing architecture of the embedded LNA as shown in Fig. 4. In the self-healing mode, an external feedback is enabled across the LNA such that this feedback causes the LNA to oscillate and produce a sinusoidal signal for testing and calibration purposes. The feedback network is a simple phase shifter and can be implemented on-chip or off-chip on the load-board. The phase-shifter is connected to the input and output ports of the LNA by switches to complete the feedback loop. The sinusoidal signature from the LNA output is down-converted and the FFT of the down-converted signal is computed in the base-band DSP to determine the oscillation frequency of the LNA with the enabled feedback. It is seen from Fig. 4 that all of the above can be accomplished *without the use of any external RF test stimulus*. Self-healing of the LNA in the presence of process variations is achieved by adjusting the LNA performance tuning "knobs" using on-chip RF mixer, ADC, low-pass filter, image reject filter and DSP resources that are necessary for performing normal wireless communication functions.

In the proposed architecture, a phase shifter is designed in such a manner that:

(a) After inclusion of the external feedback, the LNA oscillates around the desired operating or testing frequency.

(b) The oscillation frequency of the LNA with the included external feedback is sensitive to process variations and differs significantly for the golden LNA and LNAs with parametric failures.

(c). The phase shifter design is robust to manufacturing process variations and may be located on the load-board outside the chip (allowing its performance to be controlled accurately).

(d). The change in the oscillation frequency due to parametric defects in the LNA is measurable by the receiver chain (must lie within the bandwidth of the receiver chain and be detectable using the on-chip ADC's sampling speed and resolution).

In our experiments, estimation of the maximum ($F_{max}$) and minimum ($F_{min}$) change in the oscillation frequency due to parametric defects around the desired testing frequency ($F_0$) is performed using Monte Carlo simulations. In practice, oscillation frequency measurements made on LNA samples selected from different production lots and across a large number of wafers are used to determine the values of $F_{max}$ and $F_{min}$. The presence of a band-pass filter after the LNA works as an image-reject filter and helps to avoid misclassification of a faulty LNA as a good LNA because of the down-conversion of the output signal of the LNA.

### C). Classification of Catastrophic and Parametric Failures

In the proposed test method, feedback from a phase-shifter causes the embedded LNA to oscillate according to the well known Barkhausen criterion [6] provided the forward transmission gain (*S21cascade*) of the system (Fig. 5) is such that $|S21cascade| \geq 1$ and the phase of $S21cascade = 0$ degree.

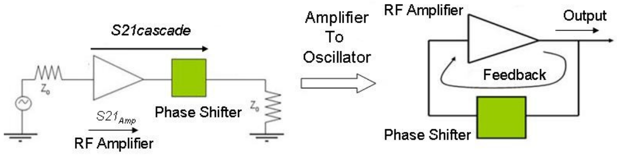

Fig. 5. Conversion of an amplifier into an oscillator.

The defects in the LNA cause changes in its forward transmission gain ($S21_{Amp}$), hence the oscillation frequency of the system changes around the oscillation frequency of the "golden" LNA. In our approach, the phase shifter is designed in such a way that catastrophic defects in the LNA cause no oscillations to occur while parametric defects lead to a change in the oscillation frequency of the LNA (with feedback) around the response of the golden LNA. The specifications of the embedded LNA are predicted from the change in the oscillation frequency using a non-linear prediction model that maps the observed change in the oscillation frequency of the DUT to changes in its performance specifications. A nonlinear prediction model based on Multivariate Adaptive Regression Splines (MARS) has been used in this paper. Details regarding MARS can be found in [7]. Previously MARS has been demonstrated for mixed-signal/RF testing in [8]. The development of a prediction model using MARS is a supervised learning process and requires a "training set" of LNAs with statistically likely parametric failures. The training set used to estimate the maximum ($F_{max}$) and minimum ($F_{min}$) change in the oscillation frequency due to parametric defects around the desired testing frequency ($F_0$) is used for the development of the prediction models. The oscillation frequency is used as a test-signature ($f_{osc}$) to predict the performance of the LNA ($S_s$) according to Equation (1).

$$S_s = F_{ms}(f_{osc}).\, f_{osc} \quad \ldots\ldots (1)$$

where,

$F_{ms}$ is non-linear regression function of the weighted sum of basis functions made of splines,

As discussed earlier, LNAs for which oscillations do not occur are considered to have catastrophic failures, while LNA samples which result in oscillations are assumed to have parametric failures. Self-healing of the LNAs (with parametric failures) is performed by adjusting the tuning knobs of the DUT according to the tuning procedure described below.

### D). Tuning Knob Selection and Self-Healing Procedure

Self-healing RF circuits require the design with "calibration/tuning knobs" through which their performance can be controlled post-manufacture, by adjusting the tuning knob values. Tuning knob control algorithms must also be devised that allow the performance specifications of RF circuits to be compensated to the maximum extent possible using such post manufacture tuning knob control. In the best scenario, the design of tuning knobs that can control the specifications of a DUT *independent* of other specifications is encouraged. This allows all specifications to be controlled independently post manufacture, allowing maximum yield recovery. However, in analog/RF circuits, different performances of the circuits are *interdependent*, thereby making it nearly impossible to find tuning knobs which satisfy the above property. For particular applications, certain specifications of RF circuits are important while others are not. For example, Gain specification of the LNA can be stringent in certain applications, while other specifications (such as P1dB and Noise Figure) have sufficient performance margins. In this case, a tuning knob can be introduced to vary the Gain of the LNA with less concern for P1dB and Noise Figure. For multi-specification tunable design, multiple tuning knobs may be necessary and optimal tuning solutions should be found to meet yield criteria.

The calibration process can be a one-time or iterative tuning procedure. In the iterative process, the tuning knobs are adjusted and measurements made at each iteration until the required specifications of the DUT are achieved. This procedure gives high yield recovery but is time consuming. In the one-time tuning procedure, after analyzing the response of the DUT, the tuning knobs are programmed only once.

In this paper, we have investigated the one-time tuning procedure which works as follows. After the specifications of the DUT are predicted using the non-linear prediction model, the DUT tuning knobs are adjusted using the *performance curves* of the DUT and Equation (2). The *performance curves* of the DUT show the changes in the specifications of the DUT as functions of the DUT tuning knob values (one function for each DUT specification) and are obtained by changing the tuning knob values of the golden DUT and observing how its performance specifications are affected. To estimate the change in each specification of the DUT, the weighted sum of the effect of each DUT tuning knob is computed according to Equation (2). Equation (2) is a first-order linear approximation of the effect of multiple tuning knob perturbations on each specification of the DUT. For multi-specification optimization, a set of such linear simultaneous equation can be solved.

$$\Delta S_j = \sum w_i \Delta K_i \quad \ldots\ldots (2)$$

where,

$\Delta S_j$ is required compensation in the specification "j"

$w_i$ is weight associated with the change in the tuning knob ($\Delta K_i$).

To illustrate, let us consider embedded LNA with two knobs, Knob1 and Knob2. Knob1 tunes a capacitance in the LNA and Knob2 tunes power supply of the LNA. The change in the Gain of the LNA because of the change in power supply and capacitance in the LNA is shown in Fig. 6. Then, the compensation in the gain (ΔG) can be performed vs equation (3).

$$\Delta G = m_1 .\, \Delta C + m_2 .\Delta Vdd \quad \ldots\ldots (3)$$

where,

$m_1$ and $m_2$ can be approximated to the slope of the performance curves in Fig. 6A and Fig. 6B respectively.

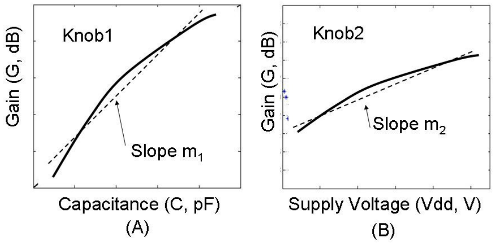

Fig.6.The performance curves of LNA for different calibration knobs.

For, efficient working of this tuning procedure, the tuning knobs should be chosen so that the specifications of the DUT vary almost linearly with the tuning knob values (even in the presence of nonlinearities in the DUT, the linear assumption gives yield improvement as shown in the following sections). Further, as stated earlier, the tuning knobs can be chosen such that each DUT specification is largely dependent on only one knob. In that case, Equation (2) reduces to $\Delta S_1 = w_1.\Delta K_1$.

## III. SIMULATION

To demonstrate the proposed self-healing methodology, a 900 MHz cascode LNA (Gain = 9.5 dB, P1dB = -3.38 dBm) with source degeneration was designed in CMOS 0.18 um process. In this LNA, two tuning knobs have been introduced - one to change the capacitance ($C_{cap}$) in the LC tank and the other to change the power supply ($V_{dd}$). Fig. 7.A shows the simulation setup in which the feedback is applied to the LNA using a phase shifter such that the LNA becomes unstable and starts oscillating. This enables the generation of test signature without any input test stimulus. In this test-setup the phase-shifter is designed such that no oscillation occurs for catastrophic failures while oscillation frequency shifts for the parametric failures around the response of the golden LNA.

For illustration, 10 single-catastrophic failures (5 open and 5 short) were introduced at 5 nodes of the LNA and 100 parametric instances of the LNA were generated by randomly perturbing LNA components including inductors, capacitors and transistors using Monte Carlo simulations. It is assumed that all the components follows Gaussian distribution (3-sigma = 5%). Also, it is assumed that each type of component has similar variations, but their variations from different components are independent. For example, all capacitors are assumed to have similar variations, but their variations are independent from those of transistors and inductors. Simulations were performed in Advance Design System (ADS) tool and the sinusoidal signal at the output of the LNA was down-converted using a behavioral model of a RF-mixer, a low-pass filter and a band-pass filter in the Matlab as shown in Fig. 7.B. Also, all DSP processing were done in Matlab.

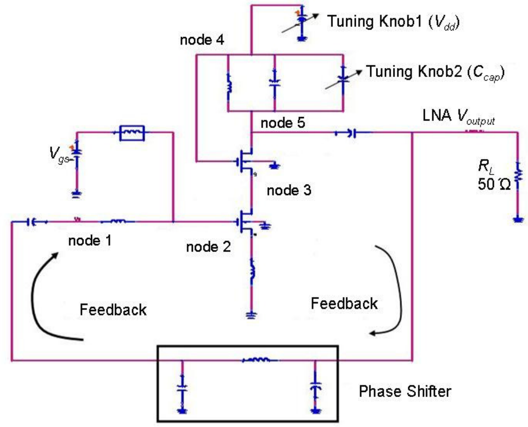

Fig.7A. LNA Modeling.

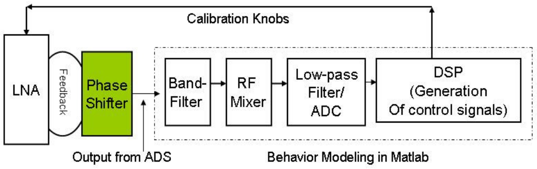

Fig.7B. RF system modeling.

Fig.7. Simulation Setup of the proposed method.

The down-converted oscillation frequency of all the 110 samples of the LNA (with 100 parametric and 10 catastrophic defects) is shown in Fig. 8. It is can be inferred from the Fig.8 that for some of the LNAs no-oscillations have occurred, while for others the oscillation frequency is around the response of the golden LNA. It is important to note that no-oscillation has occurred for the LNA with catastrophic defects. Thus, depending on the occurrence of the oscillation, the LNA with parametric variations can be separated from LNAs with catastrophic defects.

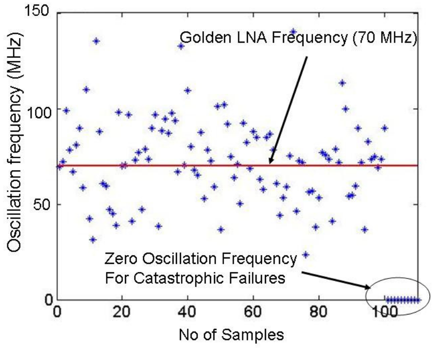

Fig.8. Oscillation frequency of the various LNA samples.

To determine which samples of LNAs should be chosen for self-correction/calibration, a non-linear prediction model to predict the forward transmission gain (Gain, dB) and 1-dB compression point (P1dB, dBm) was developed using MARS. The prediction model was developed using the training set which had 450 LNAs. The 450 LNAs were obtained by randomly perturbing components of LNA using Monte Carlo simulations. The predicted Gain and P1dB of the 100 samples of the LNA is shown in Fig. 9A and Fig. 9B, respectively.

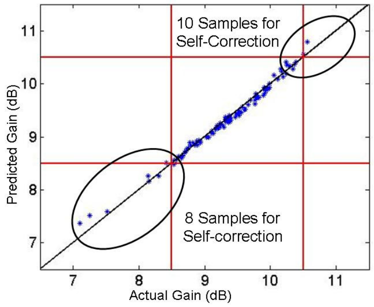

Fig.9.A. Prediction of Gain.

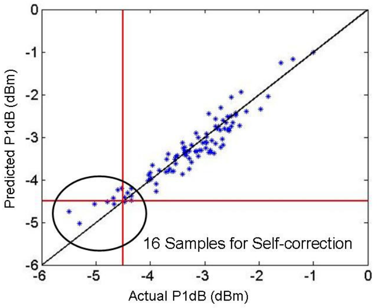

Fig. 9.B. Prediction of P1dB.

Fig.9. LNA analysis of parametric failures.

It is can be seen from the results shown in Fig. 9, that the predicted performance of the LNA from the self-generated test signature is quite accurate. Thus, this method can be used for self-testing of LNAs. Let us assume that the allowable performance specification of Gain is from 8.5 dB to 10.5 dB and P1dB should be more that -4.5 dBm. Considering an error in the prediction at the boundary of the allowable specifications, 18 samples are selected for calibration to meet Gain specification and 16 samples to meet P1dB specification.

The self-correction/calibration is done with the help of two tuning knobs. First tuning knob (Knob1) changes power supply ($V_{dd}$) of the LNA and second tuning knob (Knob2) changes the capacitance ($C_{cap}$) in the LC tank in the LNA. The variable capacitance can be implemented using varactor or choosing capacitor from bank of embedded capacitors. As a proof of concept, we have shown that the performance of the LNA can be varied by changing the capacitance in its LC tank.

The performance curves of the LNA with respect to these two tuning knobs, Knob1 and Knob2, are shown in Fig. 10 and Fig.11. For yield improvement, the change in tuning knobs was calculated using Equation (2) and predicted value of the specification from the regression model is used to calculate $\Delta Sj$. For all the calibrations, the change in capacitance ($\Delta C_{cap}$) is in the range of ± 0.6 pF and the change in power supply ($\Delta V_{dd}$) is in the range of -0.07 V to 0.24 V.

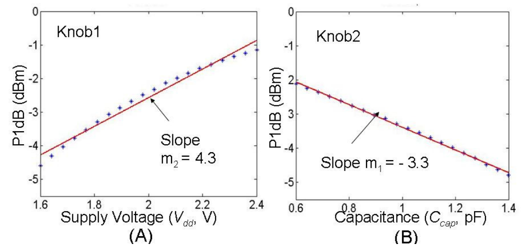

Fig. 10. Performance curves: P1dB of LNA as a function of the tuning knobs.

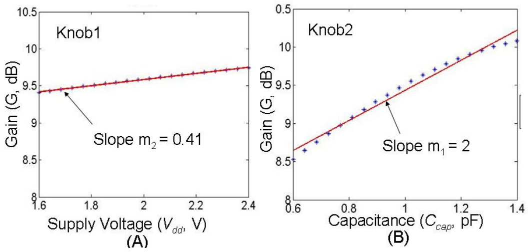

Fig. 11. Performance curves: Gain of LNA as a function of the tuning knobs.

### A). Calibration using single Knob for P1dB

In this sub-section, the proposed calibration methodology is applied to 16 samples of the LNA to increase their P1dB above - 4.5 dBm and only one calibration knob, Knob1, was used. The specification distribution before and after calibration is given in Fig. 12 and the summary of the results is given in Table I.

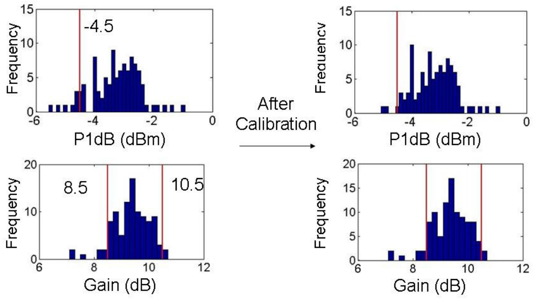

Fig. 12. Specification distribution before and after calibration using Knob1.

TABLE I: SUMMARY OF CALIBRATION RESULTS (KNOB 1)

| | % of LNAs with Gain (8.51– 10.49 dB) | % of LNA with P1dB (> -4.49 dBm) | Yield of LNA (Gain and P1dB) |
|---|---|---|---|
| Before calibration | 91% | 92% | 85% |
| After Calibration | 91% | 98% | 91% |

The obtained results show that after calibration only 2% samples are not meeting P1dB specification. However, distribution for Gain has not improved. To increase number of LNA samples with in allowable tolerance of the Gain, the calibration for the Gain is explored in the next sub-section.

### B). Calibration using single Knob for Gain

In this sub-section, the LNA samples were calibrated using Knob2 with focus on improving Gain. The obtained results are shown in Fig.13 and summarized in Table II.

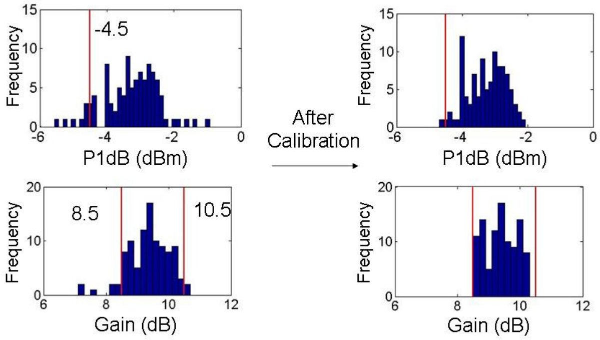

Fig. 13. Specification distribution before and after calibration using Knob2.

TABLE II: SUMMARY OF CALIBRATION RESULTS (KNOBS 2)

| | % of LNAs with Gain (8.51 – 10.49 dB) | % of LNA with P1dB (> -4.49 dBm) | Yield of LNA (Gain and P1dB) |
|---|---|---|---|
| Before calibration | 91% | 92% | 85% |
| After Calibration | 100% | 98% | 98% |

The above results show improvement in Gain yield to 100%, but P1dB yield is still 98%. Hence, to get better yield of LNA, calibration was done using both the knobs.

### C). Calibration using both the Knobs

In this calibration process both knobs were used and obtained results are shown in Fig. 14. Samples which were not meeting both Gain and P1dB specifications were calibrated using both the knobs and change in the calibration knobs was calculated by solving two equations ($\Delta G = 2^* \Delta C_{cap} + 0.41^*.\Delta V_{dd}$, $\Delta P1dB = -3.3^*\Delta C_{cap} + 4.3^*.\Delta V_{dd}$). Samples which were not meeting P1dB alone were calibrated using Knob1 and Knob2 was used for calibrating samples which were not meeting Gain alone.

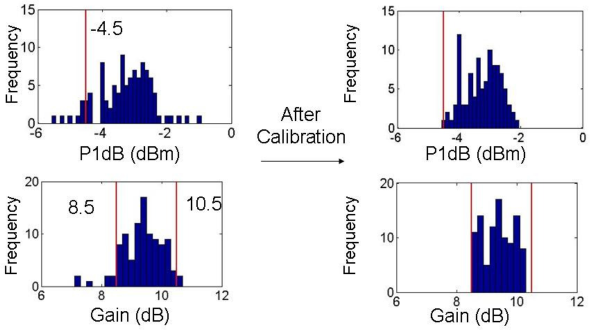

Fig. 14. Specification distribution before and after calibration using Knob1and Knob2.

TABLE III: SUMMARY OF CALIBRATION RESULTS (BOTH KNOBS)

| | % of LNAs with Gain (8.51 – 10.49 dB) | % of LNA with P1dB (> -4.49 dBm) | Yield of LNA (Gain and P1dB) |
|---|---|---|---|
| Before calibration | 91% | 92% | 85% |
| After Calibration | 100% | 99% | 99% |

Based on the results shown in Table III, it can be concluded that the yield of the LNA has increased from 85% to 99% by the proposed methodology.

## IV. HARDWARE PROTOTYPE

As a proof of concept, a hardware prototype of the proposed self-healing LNA has been made using commercially available LNA (RFMD 2411) as shown in Fig. 15. To change the performance of the LNA a single tuning knob that varies the power supply ($V_{dd}$) is used. Three samples of the LNA were considered and it was assumed that the golden sample is LNA1. Also, it is assumed that the allowable performance specification of the Gain (@875 MHz) is from 10.50 dB to 12.50 dB. The performance curve of the LNA (Gain vs $V_{dd}$) is shown in Fig. 17. The output oscillation frequency of the hardware prototype is shown in Fig. 16 at $V_{dd}$ = 3.5 V. The measured gain for LNA3 is 10.43 dB, LNA2 is 11.77 dB and LNA1 is 11.56 dB.

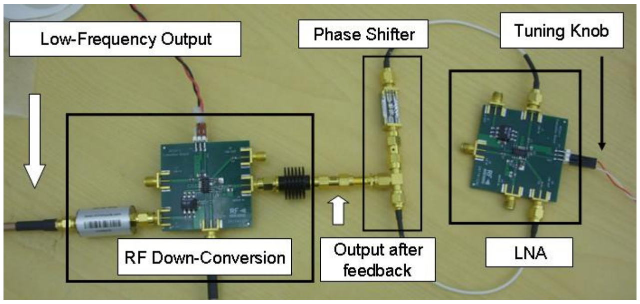

Fig. 15. A hardware prototype of the proposed self-healing LNA.

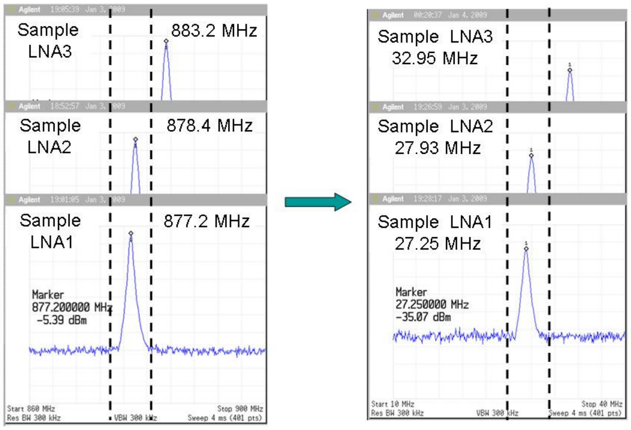

High-Frequency Signature (Output After Feedback)

Low-Frequency Output (Proposed Prototype Output)

Fig. 16. Spectrum of the output after the feedback loop and after the down conversion.

Let us assume that the prediction model to predict the gain of the LNAs is made as explained in Section II and predicted gain for LNA2 and LNA3 is 11.00 dB and 10.00 dB, respectively. Hence, by the proposed methodology, the power supply ($V_{dd}$) voltage that needs to be changed will be given by the below equation

$$\Delta G = 1.0*\Delta V_{dd} \ldots\ldots\ldots\ldots\ldots\ldots\ldots\ldots\ldots\ldots\ldots \quad (4)$$

Where m = 1.0 (Fig. 17). Let the target value of the Gain for which both the LNAs need to be calibrate is 11.5 dB. Then tuning knob for LNA2 should be changed by 0.5 V and for LNA3 it should be changed by 1.5 V

After tuning, the Gain of the LNA2 was measured as 12.25 dB and that of LNA3 was measured as 11.49 dB which are in range of expectable limit of the LNAs Gain. Hence, this experiment demonstrates that by tuning the knob of this self-healing LNA, the performance of the LNA can be changed and it can be used to increase their manufacturing yield.

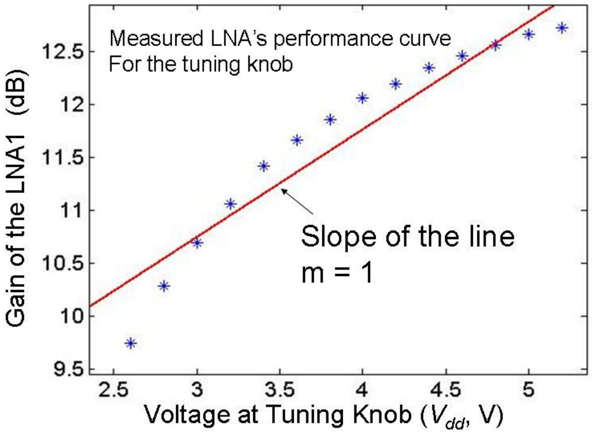

Fig. 17. Performance curve: Gain of LNA1 as a function of the tuning knob.

## V. CONCLUSION

In this paper, a new self-healing methodology has been proposed. The methodology has been demonstrated on an embedded RF LNA in the RF front-end. It has been shown through simulations that a significant yield improvement of the LNA can be achieved by using this methodology. A hardware prototype of the self-healing LNA has also been demonstrated. Based on the obtained results, it is possible to conclude that the proposed method can be considered as a promising solution for the development of self-healing systems.

## REFERENCES

[1] 2007 Edition of the International Technology Roadmap for Semiconductors (ITRS).

[2] R. Goering and R. Wilson, Yield, packages hang up design below 100nm, EE Times, March 31, 2003.

[3] T. Das, A. Gopalan, C. Washburn, and P.R. Mukund, “Self-calibration of input-match in RF front-end circuitry,” IEEE Trans. Circuits and Systems, vol. 52, no. 12, Dec. 2005, Pages (s): 821-825,

[4] D. Han, B. S. Kim, A. Chatterjee,“DSP Driven Self-Tuning of RF Circuits for Process-Induced Performance Variability ”, IEEE Trans. on Very Large Scale Integration (VLSI) Systems. pp (accepted).

[5] K. Arabi, B. Kaminska,"Oscillation built-in self test (OBIST) scheme for functional and structural testing of analog and mixed-signal integrated circuits", IEEE Proc. International Test Conference, 1997.Nov. 1997 Page(s):786 – 795.

[6] R. G. Rogers, Low Phase Noise Microwave Oscillator Design, Artech House, Inc 1991.

[7] J. H. Friedman, “Multivariate adaptive regression splines,” The Annals of. Statistics,vol. 19, no. 1, pp. 1–141. 1991.

[8] R. Voorakaranam, S. Cherubal, and A. Chatterjee, “A signature test framework for rapid production testing of RF circuits,” IEEE Proc. Design Automation and Test in Europe, March 2002,Page(s): 186 – 191.